

Novel approach combining physico-chemical characterizations and mass transfer modelling of nanofiltration and low pressure reverse osmosis membranes for brackish water desalination intensification

M. Pontié^{a*}, H. Dach^{a,b}, J. Leparc^c, M. Hafsi^d, A. Lhassani^b

^aUniversity of Angers, Group Analysis and Processes (GAP), 2, Bd. Lavoisier,
49045 Angers Cedex 01, France

Tel. +33-2-41 735207; Fax +33-2-41 735352; email: maxime.pontie@univ-angers.fr

^bFaculty of Science and Technology, Laboratory of Applied Chemistry, P.O. Box 2202, Fez, Morocco

^cVeolia Water, Anjou Recherche, Chemin de la Digue, BP 76, 78603 Maisons-Laffitte, France

^dONEP, Morocco

Received 17 December 2006; accepted 3 January 2007

Abstract

The aim of the present work is to establish a systematic approach in the range of characterization of commercial nanofiltration (NF) and low pressure reverse osmosis (LPRO) membranes materials for a better help to the users. We developed two sorts of characterizations: (i) first *physico-chemicals* in terms of hydrophobicity/hydrophilicity, morphology and topography and (ii) secondly by mass transfer in terms of pure water and saline solution permeabilities, monovalent (NaCl) and divalent (Na₂SO₄) solutes rejections and molecular weight cut-off determination. A model inspired by the phenomenological approach proposed by Kedem and Katchalsky (KK) and completed by Spiegler (S) will help us to quantify separately both parts of mass transfer occurring, the pure convection or advection and the pure diffusion for three membranes in polyamides, 2 NF and 1 LPRO, denoted NF270, NF90 and BW30, respectively, purchased from Dow. We have limited our study to low concentration polarization by using diluted solutions (10⁻³ to 10⁻¹ M) and high flow rate (4 m s⁻¹) under low conversion (5%) operational conditions to develop a new and original approach to classify and better understand the behavior of the commercialized NF and LPRO membranes under brackish waters in order to guide the users to find a suitable membrane.

Keywords: Nanofiltration; Low pressure reverse osmosis; Characterizations; SKK mass transfer; Selectivity; Brackish water; Drinking water defluorination

*Corresponding author.

Presented at the conference on Desalination and the Environment. Sponsored by the European Desalination Society and Center for Research and Technology Hellas (CERTH), Sani Resort, Halkidiki, Greece, April 22–25, 2007.

1. Introduction

The nanofiltration (NF) membrane is a type of pressure-driven membrane which properties is situated between reverse osmosis (RO) and ultrafiltration (UF) membranes. NF offers several advantages such as low operational pressure, high flux, high retention of multivalent anion salts and organics compounds with molecular weight above 300 Da, relatively low investment and low operation and maintenance costs. Because of these advantages, the applications of NF worldwide have increase. The history of NF dates back to the 1980s when RO membranes with a reasonable water flux operating at relatively low pressures were developed. Hence, the high pressures traditionally used in RO resulted in a considerable energy cost. Thus, membranes with lower rejections of dissolved components, but with higher water permeability, would be a great improvement for separation technology. Such low-pressure RO membranes became known as NF membranes. By the second half of the 1980s, NF had become established, and the first applications were reported as detailed in a recent review [1]. Today 10% of brackish waters market in the world is dedicated to nanofiltration (NF) membranes [2]. While nanofiltration is a relatively new membrane process, it is already widely used for water treatment in different parts of Europe, Israel and the US. Striving towards improved quality, efficiency and applicability, research is continuing in an attempt to understand and model the varying parameters involved during NF. A technique that is often used for the evaluation of membranes is the flux and rejection behavior of uncharged and charged solutes [3]. However, many membranes have to be screened in order to find a suitable membrane.

NF is used when high molecular weight solutes have to be separated from a solvent. It is effective in the production of drinking water, especially in the case of water softening. Compared to RO a lower retention is found for monovalent ions.

But very recently [4] it has been found that the polyamide NF45 membrane separates the ions of the same valency for a selective defluorination of brackish water. RO and ultra-filtration (UF) have shown, respectively, solution-diffusion and convection mass transfers. In NF a synergism between both can be observed but strongly depends on the operational conditions (pH, ionic strength, flow rate, transmembrane pressure) and on the membrane material.

The aim of the present work is to establish a systematic approach in the range of commercial nanofiltration characterization and low pressure reverse osmosis membranes in order to guide the user to find a suitable membrane.

The first part is dedicated to the characterizations of two NF membranes, denoted NF270, NF90 in comparison to a LPRO membrane, denoted BW30. All membranes materials are in polyamide. We will give two sorts of characterizations: (i) physico-chemicals from contact angle and AFM experiments, and (ii) mass transfer analysis from the SKK model for water and synthetic salt solution permeabilities measurements. The selectivity is follow from the retention vs. pressure and ionic strength for NaCl and Na₂SO₄ electrolytes solution in order to determine the following mass transfer parameters such as σ the reflection coefficient, C_{conv} the convective part of the solute transport, J_{diff} the diffusional part of the solute transfer P_M solute permeability and the molecular weight cut-off from Na₂SO₄ rejections.

In a second part we will present preliminary results dedicated to the comparison of two nanofiltration membranes, the NF270 and NF90 membranes, for the defluorination of a high-fluorinated brackish water from the endemic region of Fatick, Senegal (west Africa).

2. Theory

The transport of solutes through a membrane can be described by using the principles of irreversible thermodynamics (IT) to relate the fluxes

with the forces through phenomenological coefficients. For a two components system, consisting of water and a solute, the IT approach leads to two basic equations [5]:

$$J_v = L_p [\Delta P - \sigma \Delta \Pi] \quad (1)$$

$$J_s = P_s \Delta C_s + (1 - \sigma) J_v C_{\text{int}} \quad (2)$$

where J_v and J_s are respectively the solvent flux and the solute flux, ΔP and $\Delta \Pi$ define respectively the pressure and osmotic differences between each side of the membrane, L_p is the hydraulic permeability to pure water, σ is the local reflection coefficient, P_s is the solute permeability, and C_{int} is the solute concentration in the membrane and $\Delta C_s = C_m - C_p$ with C_m and C_p the concentrations respectively at the surface of the membrane in the bulk side and in the permeate. We have also defined in the following text L'_p the hydraulic permeability for a saline solution and P_c the critical pressure defined as

$$P_c = \sigma \Delta \pi: \text{critical pressure (kPa)}$$

The parameter P_c is the efficient pressure for which the first droplets of water are observed in the permeate.

With constant fluxes, constant transport parameters (L_p and σ), integration of Eq. (2) on the membrane thickness yields, in term of the real salt rejection, give the following rejection expression [6]:

$$R = \frac{\sigma(1 - F)}{1 - \sigma F} \quad (3)$$

$$\text{with } F = e^{-\frac{1-\sigma}{P_s} J_v} = e^{-\frac{1-\sigma}{P_M} J_v}.$$

From Eq. (3), it appears that the retention increases with increasing water flux and reaches a limiting value σ at an infinitely high water flux, as recently reported [4]. As the diffusive flux of the solute can be neglected in the range of the higher water flux, the reflection coefficient σ is

a characteristic of the convective transport of the solute. A σ value of 100% means that the convective solute transport is totally hindered or that no transport by convection takes place at all. This is the case for ideal RO membranes where the membranes have dense structure and no pores are available for convective transport. Eq. (3) however only relates the membrane surface concentration to the permeate concentration. It needs to be combined with concentration polarization if the permeate concentration is to be related to the bulk feed concentration which results in the combined film theory — Spiegelner–Kedem [7].

According to the *film theory*, the relation between the observed rejection rate and the true rejection R may be expressed as

$$L_n \left(\frac{1 - R_{\text{obs}}}{R_{\text{obs}}} \right) = L_n \left(\frac{1 - R}{R} \right) + \frac{J_v}{K} \quad (4)$$

where K is the mass transfer coefficient.

Substitution of Eq. (3) into Eq. (4) and rearranging results in the following equation [7]:

$$R_{\text{obs}} = \frac{1}{\frac{1 - \sigma}{\sigma \left(1 - e^{-\left(\frac{1 - \sigma}{P_M} \right) J_v} \right)} e^{\frac{J_v}{K}} + 1} \quad (5)$$

By using a nonlinear parameter estimation method by supplying the data of R_{obs} vs. J_v taken at different pressures but at constant feed rate and constant feed concentration for each set, Eq. (5) may be used to estimate the membrane parameters σ and P_M and the mass transfer coefficient, K , simultaneously [6]. A wide variation of transmembrane pressure at a constant feed flow rate are required to prevent poor regression due to too many unknowns (σ , P_M and K) compared to the experimentally obtainable variables (J_v and R_{obs}). Even in this case, poor regression might still be obtained for high values of K . In this particular case, the inequality $K \gg J_v$ olds

at most values of J_v and this prevent to obtained K with some confidence because $R_{\text{obs}} = R$ (Eq. (5) reduces to Eq. (3) for any value of $K \gg J_v$). To the author opinion the best way to determine the σ and P_M values is to work under experimental conditions so that $K \gg J_v$ (high tangential rate and low pressure). This allows to directly obtaining the true rejection and then σ and P_s using a nonlinear least squares estimation procedure that makes Eq. (5) fit the data as closely as possible.

An other way to quantify the convective and diffusive parts is to expressed Eq. (2) as

$$J_{\text{diff}} + J_v C_{\text{conv}} = C_p J_v$$

where J_{diff} is the solute flux due to diffusion (with $J_{\text{diff}} = P_M \Delta C_s$), and C_{conv} is the solute concentration due to convection [with $C_{\text{conv}} = (1 - \sigma)C_{\text{int}}$].

Note that this equation is identical to the Kedem–Katchalsky model and does not imply a linear concentration gradient as it is frequently reported. It may be expressed as well as [4,8]:

$$C_p = \frac{J_{\text{diff}}}{J_v} + C_{\text{conv}} \quad (6)$$

By following C_p vs. the reverse of the permeate flux, it is possible to quantify separately both part of the solutes mass transfer occurring in NF: convection and solvation/diffusion as developed recently [4]. The results are expected to be valid only in some limited domain of operating

conditions with low polarization concentration and with membrane considered having no charge. This approach may be useful for the comparison of the behavior of different NF and RO membranes. During our experiments we have limited the concentration polarization by using dilute solutions and high flow rate. In fact, the SKK model was developed first for uncharged membranes such as RO membranes while most NF membranes have charged, negatively or positively, depending under the physico-chemical conditions (pH, ionic strength, specific adsorption) and the kind of material employed. We have neglected the membranes charge in the present study because the membranes employed appear to have RO behavior.

3. Experiments

3.1. Membranes materials

The membranes under study are thin-film composite membranes composed of two layers as illustrated in Fig. 1; a thin polyamide film as active layer and a large mesoporous polysulfone as the support layer. The three studied membranes are 2 NF membranes, denoted NF90, NF270 and a low reverse osmosis membrane (LPRO), denoted BW30. All membranes were purchased from Filmtec (DOW, USA); the specifications of the membranes are given in Table 1. The chemical structures of the support and active layers materials are reported in Fig. 2, from Petersen [9].

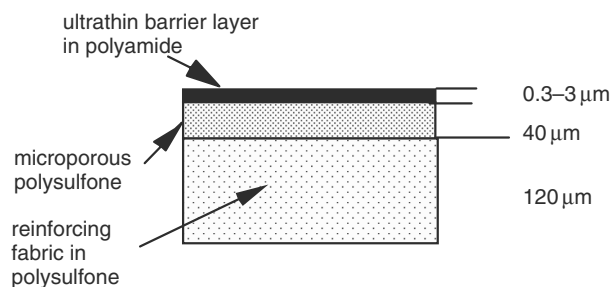


Fig. 1. Schematic diagram of the thin film composite membranes.

Table 1
NF and LPRO membranes properties from the supplier

	NF270	NF90	BW30
Supplier	Filmtec (DOW)	Filmtec (DOW)	Filmtec (DOW)
Max. temp (°C)	45	35	45
Pressure range, bar	0–41	0–41	0–41
pH range	3–10	3–9	2–11
NaCl rejection (%) ^a	40–60	85–95	99.5
Product name	NF270-400	NF90-400	BW30-400
Material	Polyamide	Polyamide	Polyamide

^aOperational conditions not specified by the supplier.

Before use, the membranes were rinsed with UP MilliQ water (Millipore system, France) until the conductivity of the permeate remained below UP water conductivity ($<3 \mu\text{S cm}^{-1}$). The effective surface membrane area was 472 cm^2 .

All the salts used (NaCl , Na_2SO_4) were of analytical grade from Aldrich (France) and used as received. All solutions were prepared from a MilliQ water (Millipore system, France) with a purity water presenting a conductivity lower than $3 \mu\text{S cm}^{-1}$ and $\text{pH} = 6.7$. The salts analyses were carried out by a conductimeter (PHM210, from Radiometer Analytical, France) after

standardization for each salt and concentration were deduced for single salt solutions.

3.2. Bench scale pilot plant

The NF/LPRO pilot plant were supplied by Sepratech (module SEPA II, Separation Technology, INC, US), and consisted of a feed tank, a pump Wanner (Wanner GP, US) and a planar module, as detailed in Fig. 3. All studies were done using a low conversion (5%) and a high tangential flow rate ($\sim 4 \text{ m s}^{-1}$) in order to minimize the polarization concentration effects. The

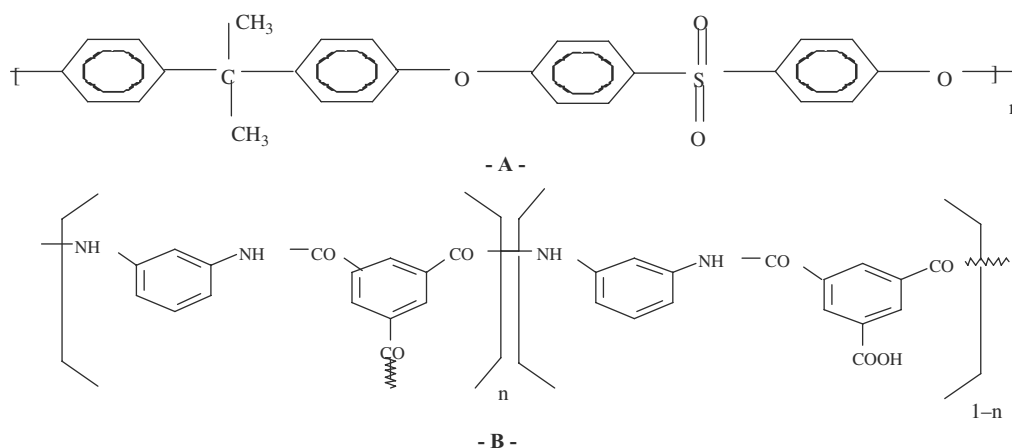


Fig. 2. Chemical structures of the support (A) and active layers (B) of the NF (NF90, NF270) and LPRO (BW30) membranes.

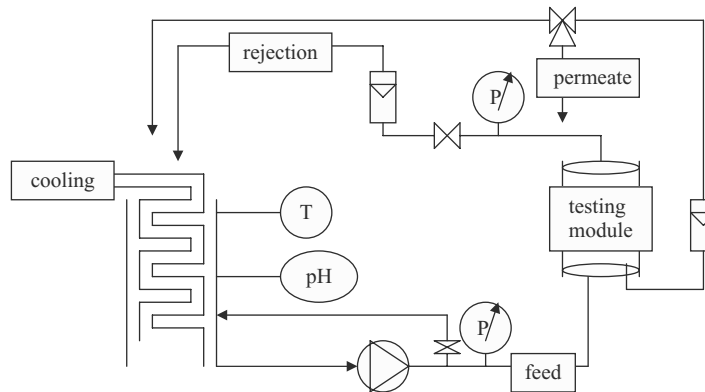


Fig. 3. Flow diagram of the NF/LPRO plant (lab-scale experiments, January–March 2005).

applied transmembrane pressures were in the range of 0–25 bar. The temperature was maintained at 25°C.

Permeated solutions were recycled during the runs except for samples withdrawn for the calculation of observed retention denoted R_{obs} according to

$$R_{\text{obs}} = 1 - \frac{C_p}{C_0} \quad (7)$$

where C_p and C_0 are the concentrations in the permeate and feed solutions, respectively. But under our hydraulic conditions we can consider that $R_{\text{obs}} = R$.

Pure water flux through a membrane can be described by the Darcy's law from the Eq. (1):

$$J_v = L_p \Delta P \quad (8)$$

with L_p the hydraulic permeability.

3.3. Contact angle measurements

The contact angle measurements were carried out by the sessile drop technique. The different membranes were primarily washed twice with deionised water for a period of 24 h and then dried at room temperature over silicagel in a desiccator. A droplet of UP milliQ water solution

(a volume of 1–2 μL) was deposited onto the surface with a microsyringe and contact angles of the droplet with the surface were measured with a KRUSS G10 contact angle meter. Reported values are the averages of the contact angles (right and left) of five droplets. During the short time of measurement (less than 1 min), no change in contact angle was observed. Contact angle do not give absolute values but allow a comparison between each materials. A variation of 2 degrees in the angle is needed to differentiate each kind of materials.

3.4. AFM experiments

AFM studies will contribute towards further improvement of the NF membranes especially for desalination of brackish water. AFM characterization of a series of commercial nanofiltration (NF) and reverse osmosis (RO) membranes of different polymer types for brackish water desalination has never previously been attempted. Thus, as reported by Hilal et al. [1], it is imperative to study the properties of these membranes and to show that the properties as characterized by AFM correlate to the process behavior. This is expected to provide substantial new insights into the influence of NF/RO membrane properties on performance, providing a database for the

selection of NF membranes to account for the complexities of brackish water to be treated.

The AFM equipments used were conducted with a Nanoscope III device from VEECO (USA). The membrane morphologies were imaged in contact mode in air with a scan rate of 1 Hz and 400×400 pixel resolution. The cantilevers used for such imaging were from Veeco, with a specified spring constant between $0.44\text{--}0.63 \text{ N m}^{-1}$ and a resonant frequency of $17\text{--}20 \text{ kHz}$. The mean roughness (denoted R_a) is the mean value of surface relative to the centre plane. The plane for which the volume enclosed by the image above and below this plane are equal and is calculated as

$$R_a = \frac{1}{L_x L_y} \int_0^{L_x} \int_0^{L_y} |z(x, y)| \cdot dx \cdot dy \quad (9)$$

where $z(x, y)$ is the surface relative to the center plane and L_x and L_y are the dimensions of the surface analyzed.

The roughness parameter depends on the curvature and size of TM-AFM tip, as well as on the treatment of the captured. Therefore, the roughness parameter should not be considered as absolute roughness values. However the same cantilever was used for all AFM images and all the AFM treated in this way.

3.5. Experiments conducted on a Senegalese water

Water composition is reported in the Table 10. This water is from the endemic region of Fatick (Senegal). We have filtrate a sample (40 L) of water across the two nanofiltration membranes previously characterized, NF270 and NF90 using the previously detail bench-scale pilot plant detailed in the Fig. 3. A high tangential flow rate ($\sim 4 \text{ m s}^{-1}$) was fixed and the temperature maintained at 25°C . The conversion ratio is fixed at 87%. The water was filtered under 7.5 bar during 10 h and fluoride ions concentration was

determined using a ionic chromatographic system (DX100 apparatus from Dionex, France).

4. Results and discussions

4.1. Characterizations of NF and LPRO membranes

4.1.1. Pure water permeabilities

The flux solvent evolution of pure water with the transmembrane pressure across NF/LPRO membranes are reported in Fig. 4. The linear evolution of fluxes with the transmembrane pressure shows that Darcy's law is verified. As expected, the hydraulic permeabilities determined from the slopes (Table 2) show higher values for NF than LPRO membranes, due to the larger pore size of the NF membranes. The NF90 membrane shows the higher hydraulic permeability with $L_p = 14.8 \text{ L h}^{-1} \text{ m}^{-2} \text{ bar}^{-1}$.

4.1.2. Saline aqueous solution permeabilities

The interest in knowing the permeability of the membranes for a salty solution is to predict the fluxes which could be obtained for a real brackish water (total salinity near 6 g L^{-1}) without fouling. This parameter is not usually given by the suppliers.

In the Fig. 5, we have reported the flow rate as a function of the transmembrane pressure (ΔP) for a NaCl solution at a concentration of $10^{-1} \text{ mol L}^{-1}$ (6 g L^{-1}) which is typical of a synthetic brackish water. The linearity observed suggests that this salty solution follows the Kedem–Katchalsky model (i.e. Spiegler–Kedem model, with pressure and osmotic linear gradients): the hydraulic permeabilities with the salt solution (denoted L_p') and the critical pressure P_c values obtained are reported in the Table 2. The P_c values show that the flux through the RO membrane (BW 30) starts under the theoretical osmosis pressure of 4.8 bar for a solution of NaCl 0.1 mol L^{-1} , suggesting that this LPRO

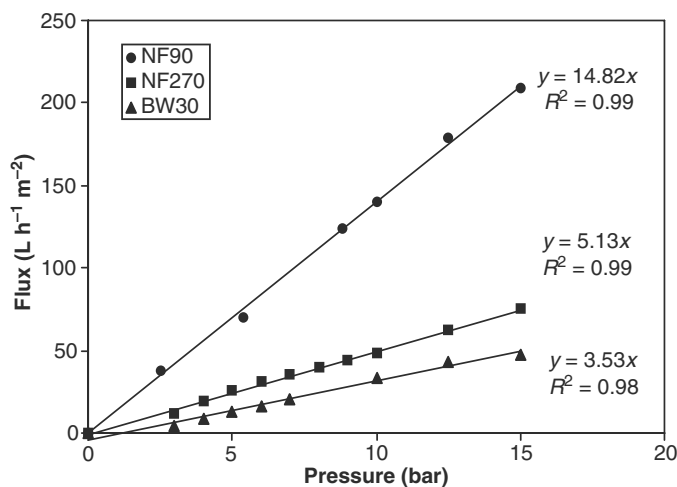


Fig. 4. Pure water flux as function of the transmembrane pressure (ΔP) for nanofiltration membranes (NF270, NF90) and low pressure reverse osmosis membrane (BW30).

membrane is more open than usual. Usually we can calculate the osmosis pressure of a NaCl solution with the formula:

$$\Pi = 48C \quad (10)$$

with C the concentration of the NaCl solution explained in mol L^{-1} .

For the NF membranes (NF90 and NF270), the critical pressure is only slightly under 2 bar and between NF and RO the osmosis pressure is lower and then NF is less limited by the osmosis pressure due to its more open pores as the LPRO membrane. For RO membranes the osmosis pressure is a solvent mass transfer limiting parameter. Finally, the interest in NF membranes in presence

of salt is their higher hydraulic permeabilities and their lower critical pressure. The NF90 membrane shows the higher hydraulic permeability with $L_p' = 5.0 \text{ L h}^{-1} \text{ m}^{-2} \text{ bar}^{-1}$ with a critical pressure of 1.6 bar.

4.1.3. Roughness of the membranes

AFM characterizations have been performed in order to determine the morphology and the topography of the studied membranes. The results obtained for 1 scan of $1 \times 1 \mu\text{m}^2$ are reported in Fig. 6. The resulting roughness for 2 scans ($50 \times 50 \mu\text{m}^2$ and $1 \times 1 \mu\text{m}^2$), are reported in Table 3. This parameter was measured by AFM itself. The mean roughness is the mean value of

Table 2

Pure water and saline solution (NaCl 0.1 M) permeabilities, contact angles and critical pressures of the NF and LPRO membranes

Membrane	$L_p (\pm 0.7) (\text{L h}^{-1} \text{ m}^{-2} \text{ bar}^{-1})$	$L_p' (\pm 0.3) (\text{L h}^{-1} \text{ m}^{-2} \text{ bar}^{-1})$	$\theta (\pm 7) (^{\circ})$	$P_c (\pm 0.1) (\text{bar})$
NF270	5.1	2.9	38	0.8
NF90	14.8	5.0	64	1.6
BW30	3.5	1.5	76	3.8

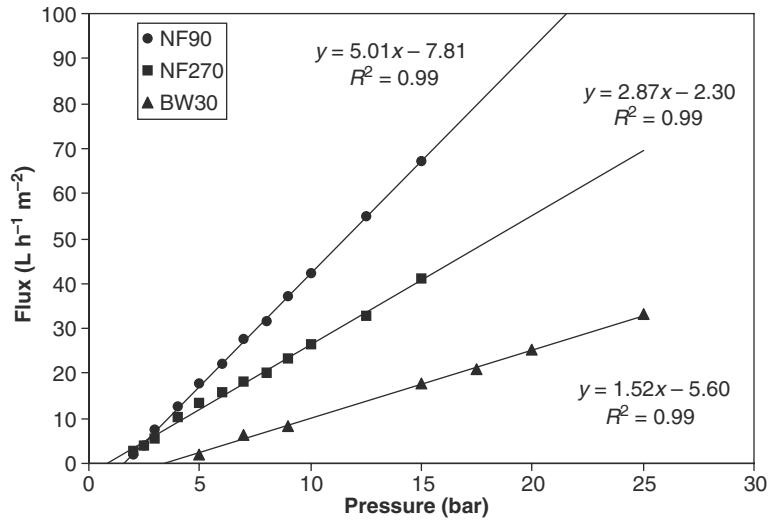


Fig. 5. Water flux of NaCl solution at 10^{-1} M as function of the transmembrane pressure for nanofiltration membranes (NF270, NF90) and low pressure reverse osmosis membrane (BW30).

surface relative to the central plane, the plane for which the volume enclosed by the image above and below this plane is equal.

It may be seen that R_a is lower for the NF270 membrane. But the more remarkable result is that the NF90 membrane present a lower roughness than the LPRO BW30 membrane. A average roughness decreases with the nominal molecular weight cut off, as recently reported [1]. The NF90 membrane shows the higher R_a with 298 ± 10 nm.

4.1.4. Contact angle measurements

In the Table 2 we have reported the results of contact angle measurements determined by the sessile drop method and conducted on dry samples. Usually, the lower is the contact angle the more hydrophilic is the material. Then, it appeared clearly that the more hydrophilic membrane surface is observed for the NF270 with a mean contact angle value of 38° . For NF90 and

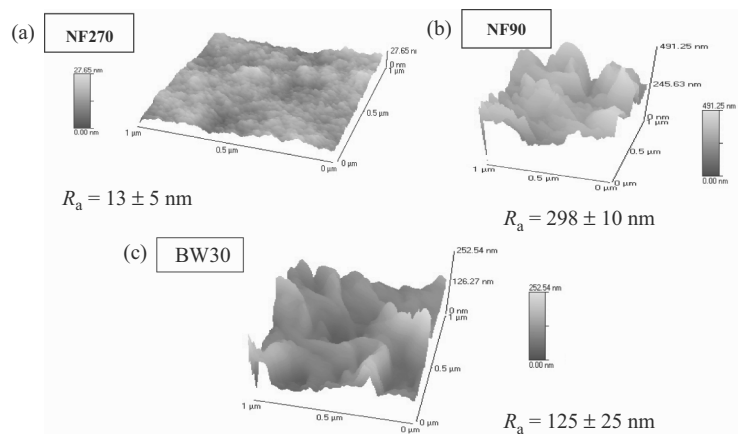


Fig. 6. 3D images of the NF270 (a), NF90 (b) and BW30 (c) membranes.

Table 3
Average roughness of NF90, NF270 and BW30 membranes

Membrane	NF270		NF90		BW30	
Field analysed	$50 \times 50 \mu\text{m}^2$	$1 \times 1 \mu\text{m}^2$	$50 \times 50 \mu\text{m}^2$	$1 \times 1 \mu\text{m}^2$	$50 \times 50 \mu\text{m}^2$	$1 \times 1 \mu\text{m}^2$
R_a (nm)	45 ± 5	13 ± 5	390 ± 20	298 ± 10	290 ± 10	125 ± 25

BW30 membranes it is more difficult to conclude because the contact angle measurements obtained might be highly influenced by their high roughnesses.

4.1.5. Determination of salt retention

Usually, to compare the performances of different membranes, the graph of the observed retention, denoted R_{obs} , as a function of the transmembrane pressure applied (ΔP) is used (see Fig. 7a). For the three membranes studied the data obtained at $\Delta P = 5$ bar and $\Delta P = 15$ bar are reported in Table 4. We observed that the BW30 membrane shows the higher retention as attempted and between the NF membranes the order observed is

$$R(\text{NF90}) > R(\text{NF270})$$

It means that the more open pores NF membrane (NF270) shows the lower retention, as also reported by the supplier. But some inversions can be observed for the retention between low pressure and high pressure. We can attribute this modification to the inversion of the predominant mass transfer occurring at low pressure and high pressure, as reported before [13]. For the divalent salt Na_2SO_4 we can observe a drastic difference between the rejections for the NF90 and BW30 membranes in comparison to the NF270. Then the NF90 membrane seems to have a behavior very similar to the BW30.

4.1.6. Hydrodynamical approach

The originality of the present approach is to build with the usual results from the usual graph following R_{obs} vs. ΔP (Fig. 7a) a new graph

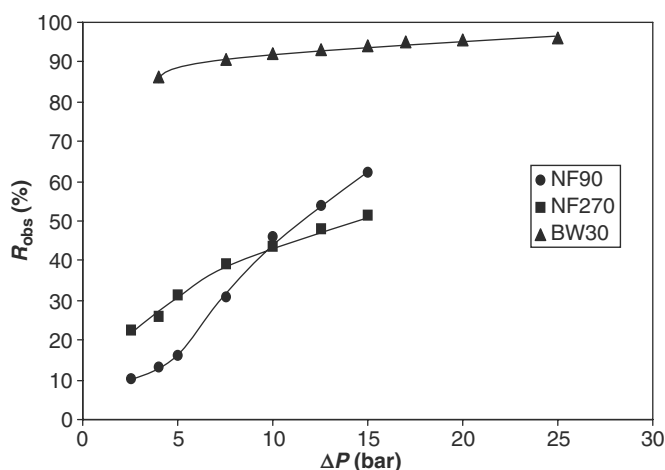


Fig. 7a. Observed retention (R_{obs}) vs. the transmembrane pressure (ΔP) (NaCl 0.001 M, pH = 6.5).

Table 4

R_{obs} values determined for NF90, NF270 and BW30 membranes under different transmembrane pressure applied and 2 salts (NaCl and Na_2SO_4)

Concentration (mol L ⁻¹)		R_{obs} (%)			
		0.001		0.1	
		$P = 5$ bar	$P = 15$ bar	$P = 5$ bar	$P = 15$ bar
NaCl	NF270	34	59	11	20
	NF90	15	62	5	50
	BW30	ND	94	ND	93
		$P = 15$ bar			
Na_2SO_4	NF270	93		60	
	NF90	99		98	
	BW30	99		98	

ND: not determined.

representing C_p as function of $1/J_v$, as illustrated on the Fig. 7b. Then, the permeate concentration as a function of the reverse permeate flow ($1/J_v$) revealed a linear evolution in conformity to the Eq. (6). For $1/J_v \rightarrow 0$ we obtained C_{conv} , the

convective part of the solute mass transport. From the slope we obtained J_{diff} , the diffusion part of the mass transfer. All the C_{conv} and J_{diff} values obtained for the NF270, NF90 and BW30 membranes are reported in the Table 5 for two salts,

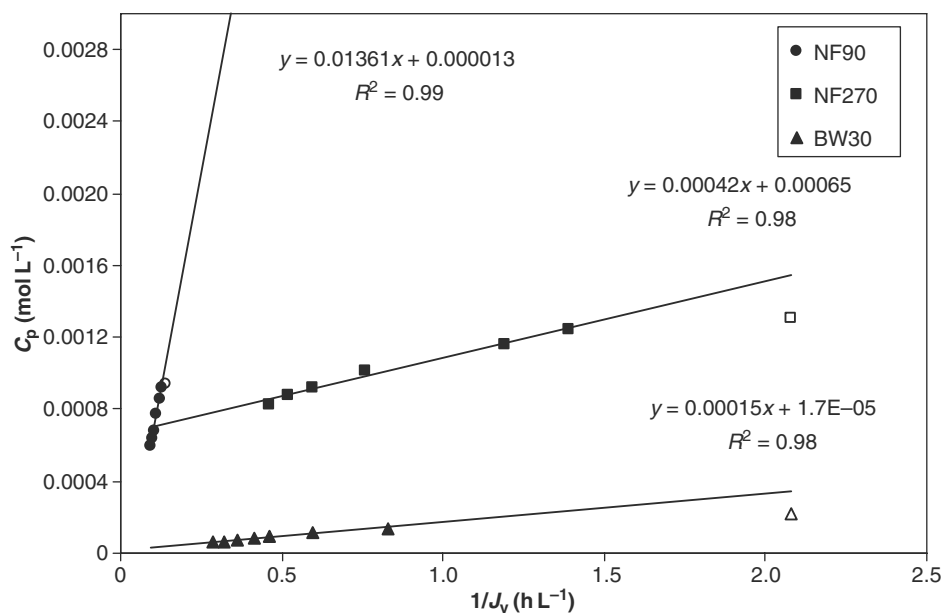


Fig. 7b. Permeate concentration (C_p) vs. the ratio $1/J_v$ (NaCl 0.001 M, pH = 6.5).

Table 5
 C_{conv} , J_{diff} values obtained from the SKK model

		C_{conv} (mol L ⁻¹)	J_{diff} (mol m ⁻² s ⁻¹)	C_{conv} (mol L ⁻¹)	J_{diff} (mol m ⁻² s ⁻¹)
Concentration (mol L ⁻¹)		10 ⁻³		10 ⁻¹	
NaCl	NF270	6.50×10^{-4}	$2.5 \times 10^{-6} (\pm 9 \times 10^{-7})$	5.02×10^{-2}	$2.5 \times 10^{-5} (\pm 1 \times 10^{-5})$
	NF90	1.37×10^{-5}	$0.8 \times 10^{-4} (\pm 8 \times 10^{-6})$	1.88×10^{-3}	$2.3 \times 10^{-3} (\pm 3 \times 10^{-4})$
	BW30	1.71×10^{-5}	$0.9 \times 10^{-6} (\pm 0.2 \times 10^{-6})$	1.71×10^{-4}	$3.5 \times 10^{-5} (\pm 1 \times 10^{-5})$
Na ₂ SO ₄	NF270	5.91×10^{-5}	$3.7 \times 10^{-7} (\pm 0.6 \times 10^{-7})$	2.91×10^{-2}	$4.2 \times 10^{-5} (\pm 0.9 \times 10^{-5})$
	NF90	1.69×10^{-5}	$7.4 \times 10^{-7} (\pm 0.5 \times 10^{-7})$	2.11×10^{-4}	$6.2 \times 10^{-6} (\pm 0.9 \times 10^{-6})$
	BW30	1.13×10^{-5}	$1.0 \times 10^{-7} (\pm 0.1 \times 10^{-7})$	7.04×10^{-5}	$3.7 \times 10^{-6} (\pm 0.7 \times 10^{-6})$

NaCl and Na₂SO₄, at two concentrations 0.1 and 0.001 M. From the C_{conv} values we can conclude that the NF270 membrane is more convective in comparison to the NF90 and BW30 membranes and for both salts studied (NaCl and Na₂SO₄). The slopes obtained confirm that NF90 membrane has a more diffusional behavior than NF270. A recent study demonstrated that diffusional NF membranes are recommended for high fluoride rejection [4]. Then we can hypothesize that the NF90 membrane will be a good candidate for the treatment of high fluorinated brackish waters.

The second part of this article will verify this prediction under a real water bulk from an endemic region in Senegal.

4.1.7. MWCO membrane determination from C_{conv} data

From the C_{conv} values obtained before and reported in the Table 5, it is possible to calculate the molecular weight cut-off (MWCO) of the three membranes studied, from the Eq. (11), as reported recently [11].

$$C_{\text{conv}} = C_0 [1 - (M/Sc)^{1/3}]^2 \quad (11)$$

with M the molecular weight of a solute, Sc the molecular weight cut off (MWCO) of the membrane and C_0 the initial concentration of the solute in the feed.

The results of the MWCO calculated are reported in Table 6. The results obtained show that the best conditions to determine the MWCO is under diluted solution (10⁻³ M) using a divalent salt such as Na₂SO₄. As observed for Na₂SO₄ rejections, it is not possible to determine a better value of MWCO at high electrolyte concentration. In the case of the NF270 we observed a rejection of 60% for Na₂SO₄ 0.1 M. This low level of rejection is not usable to determine the MWCO because the definition of the MWCO determination is based on rejections higher than 90%. Then the best well conditions are under diluted divalent salt electrolyte solution, for example at 10⁻³ M. Furthermore we attempted

Table 6
Molecular weight cut-off determined from the Eq. (16) from C_{conv} results obtained

	MWCO (Da) calculated		MWCO ^a
	Concentration Na ₂ SO ₄ (mol L ⁻¹)		
	10 ⁻³ (±20)	10 ⁻¹ (±15)	(±7) (Da)
NF270	308	2000	120
NF90	213	190	250
BW30	187	159	96

^aDetermined from the rejections of neutral calibrated compounds.

Table 7
Phenomenological parameters σ and P_M values according to sodium salts (NaCl and Na₂SO₄)

		NF270		NF90		BW30	
		Concentration (mol L ⁻¹)					
		10 ⁻³	10 ⁻¹	10 ⁻³	10 ⁻¹	10 ⁻³	10 ⁻¹
NaCl	$\sigma (\pm 0.02)$	0.43	0.26	nd	nd	0.98	0.99
	$P_s (\text{L h}^{-1}) (\pm 0.01)$	1.01	1.32	nd	nd	0.11	0.13
Na ₂ SO ₄	$\sigma (\pm 0.02)$	0.96	0.51	0.98	0.98	0.99	0.99
	$P_s (\text{L h}^{-1}) (\pm 0.01)$	0.04	0.34	0.06	0.03	0.00	0.01

the following order BW30 < NF90 < NF270, it is in good correlation with the convective properties of those membranes which is very low for the LPRO and highest for the NF270. This method is in good adequation with the order obtained using the usual method from calibrated neutral molecules. Then a new and very simple method is presented in order determine quickly the MWCO of microporous membranes.

4.1.8. Phenomenological approach

The σ and P_s values that make Eq. (5) fit the data as closely as possible are reported in Table 7. In most cases, Eq. (5) adequately describes the data (see for example Fig. 8).

As expected the higher σ values were obtained for the BW30 membrane, independently of the electrolyte solution. For the NF270 the σ values decreased when the ionic strength changes due to the decrease of the retention. For the NF90 membrane Eq. (5) does not fit the data obtained with NaCl solutions. We hypothesized that this membrane brings charges, as recently reported [12–14]. The main limit of our model is that the charge of the membrane is not taken into account. Indeed, the Donnan equilibrium should play a non-negligible role and the effect of electrostatic forces is also not negligible because they can facilitate the increase in the distribution coefficient by electric affinity increasing at the same time the diffusion part of the mass transfer. But we decided in the present study to neglect the charges bring by the studied membranes.

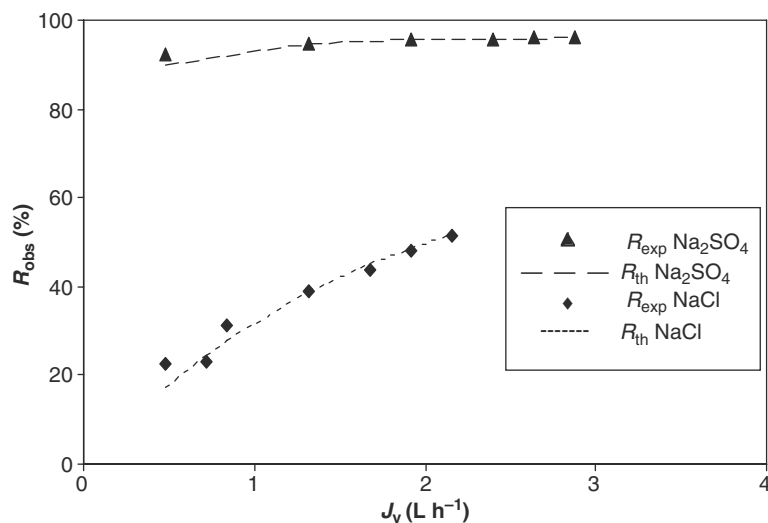


Fig. 8. Evolution of R_{obs} vs. J_v for the NF270 membrane (salts concentrations 0.001 M, pH = 6.5).

For the P_M values, if we compare the values obtained for Na_2SO_4 , we can observe the following order at low ionic strength:

NF90 > NF270 > BW30

We observed a modification between both NF membranes at high ionic strength, with the following order:

NF270 > NF90 > BW30

We can attribute this modification to a decrease of the diffuse layer thickness under ionic strength variations. It means that the NF90 membrane is less sensitive to ionic strength modifications in comparison to the NF270.

Furthermore we have to evocate the role of hydration. As reported by Pontalier et al. [25], hydration can be considered as a force, the force necessary to extract the solute from the solvent to push it into the pores. In this way, it would require more energy to extract SO_4^{2-} and to push it into the pores in comparison with Cl^- . Although this hypothesis is very difficult to confirm. But we know today more clearly that the state of the water inside the membranes differs from the bulk state in accordance to recent studies where the authors tried to obtain a water dielectric constant inside the membrane with different values simulated between 25 and 60 [15,16] with in comparison a bulk value of 78.

We have observed recently [4] that the coefficient σ , for the polyamide NF45 membrane can be correlated to the hydration energy for the halide ions, F^- , Cl^- and I^- . As a conclusion σ values seems to be highly dependent on the kind of the anion present in the electrolyte solution. Strongly solvated anions, like F^- , lead to high values of σ more than less solvated anions. That is the main interest of such nanofiltration membrane to obtain a selective defluorination. It appears clearly now that the mass transfer behavior occurring in NF dedicated to a selective defluorination

must be a NF membrane very similar in its mass transfer behavior to RO membrane.

Free water has its proper behavior concerning ions or polar molecules hydration properties. Then the solvation differences between each species for a consider membrane material show less differences between solutes between the membrane as for free water. In free water the hydration energies have higher differences between species than hydration with a membrane. Water interaction differences between solutes are higher sensitive in solution than in the membrane [17]. Then the ion rejection is mainly dependant under its hydration energy in the solution upstream and it will be more retained if it has a higher hydration energy than the others [4].

4.1.9. Comments on the C_{int} and polarization factor Φ data

From both previously developed approaches (phenomenological and hydrodynamical) we have observed that it is possible to link J_{diff} the solute flux due to diffusion with the concentration of the solute on the surface of the membrane C_m ($J_{diff} = P_M \Delta C_s = P_M (C_m - C_p)$), and C_{conv} the solute concentration due to convection with the membrane internal concentration of the solute C_{int} [$C_{conv} = (1 - \sigma)C_{int}$]. Then from C_{conv} , J_{diff} , σ and P_M we have determined C_m and C_{int} . From the C_m we have calculated the polarization factor Φ which is defined as $\Phi = C_m/C_0$. All the data obtained are reported in the Tables 8 and 9.

The lower C_{int} values are observed for the LPRO membrane due to the lower penetration of salts inside this dense RO membrane. The same behavior is observed with the NF90 membrane which has a reverse osmosis behavior as obtained before. For the NF270 the consequences of its high C_{conv} obtained is a better penetration of salts (monovalents and divalents) inside the membrane due to its more convective behavior.

Concerning the polarization factor all data obtained are situated around a value of 1 as a

Table 8
Values of C_{int} (g L^{-1}) 3 membranes and 2 salts

		Concentrations C_0 (mol L^{-1})	
		0.001	0.100
NaCl	NF270	0.0011	0.0675
	NF90	nd	nd
	BW30	0.0008	0.0170
Na_2SO_4	NF270	0.0015	0.060
	NF90	0.0008	0.010
	BW30	0.0012	0.007

nd: not determined.

consequence of the high flow rate imposed and the low conversion (5%). But it is interesting to observe that the NF270 membrane present the higher Φ values as a consequence of the higher C_{int} values observed before, specially under diluted conditions.

4.2. Application: defluorination of a natural brackish water with high level F^- from Senegal

4.2.1. Background

Fluorosis caused by high fluoride intake predominantly through drinking water containing

Table 9
Polarization factor (Φ) values determined for 3 membranes and 2 salts under various operating conditions

		Φ			
		Concentration (mol L^{-1})		0.1	
		0.001	0.1		
		Pressure (bar)			
		5	15	5	15
NaCl	NF270	0.99	0.98	0.99	0.96
	NF90	nd	nd	nd	nd
	BW30	1.14	1.11	0.99 (8 bar)	0.99
Na_2SO_4	NF270	1.24	1.3	0.88 (6 bar)	0.83
	NF90	1.01	0.99	0.46	0.41
	BW30	nd	nd	0.77 (10 bar)	0.70

F^- concentrations $> 1 \text{ mg L}^{-1}$, is a chronic disease manifested by mottling of teeth (dental fluorosis) in mild cases and changes in bone structure (skeletal fluorosis), ossification of tendons and ligaments, and neurological damage in severe cases [18–20].

Today increasing concern is being expressed that these adverse effects of fluorosis are irreversible. With the rural population of African, Indian and Chinese people in many areas currently using drinking water with high F^- concentrations supplied from wells and boreholes, the development of a long term solution for the defluorination of F^- contaminated groundwater is of critical importance. This would require appropriate water treatment procedures. Appropriate technology must be technically simple, cost effective, easily transferable, use local resources and must be accessible to the rural community.

The removal of fluoride from water using defluorination techniques is a common practice worldwide, both in industry and domestically. Current methods of fluoride removal from water include adsorption onto activated alumina, bone char and clay, precipitation with lime, dolomite and aluminum sulfate, the Nalgonda technique [21], ion exchange [22] electrocoagulation [23] and membrane processes such as reverse osmosis, electrodialysis and very recently nanofiltration [4–8]. Membrane processes such as reverse osmosis [24,25], nanofiltration, dialysis and electrodialysis are recently developed methods for F^- removal from drinking waters [24–29] and brackish waters [4,8,30].

This second part is dedicated to the presentation of recent results obtained under the comparison of two nanofiltration (NF) membranes (NF90 and NF270) processes for a selective defluorination of a Senegalese brackish water from the endemic region of Fatick (Senegal, West Africa).

4.2.2. Results and discussions

Water analysis (see Table 10) show that this water is a brackish water with a high contents in

Table 10
Fatick's water analysis (Senegal)

	F ⁻ (mg L ⁻¹)	Cl ⁻ (mg L ⁻¹)	Turbidity (NTU)	pH	Total salinity (mg L ⁻¹)
Feed water	3.76	670	0.6	8.15	2361
WHO standards	1.5	200	1	6.5–9	500

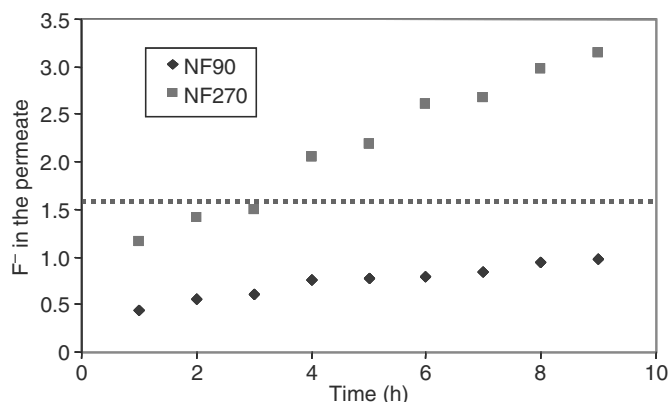


Fig. 9. F⁻ concentrations in the permeate vs. time during the filtration of the Fatick water on the NF90 and NF270 membranes (feed composition: see Table 9; operational conditions: transmembrane pressure 7.5 bar; conversion ratio 0.87, flow rate: 4 m s⁻¹).

fluoride ions in comparison to WHO standards. All the results are reported in the Fig. 9. As well detailed the evolution of the fluoride contents in the permeate increase as the following order: NF270 > NF90 > BW30. Then we can conclude that the best membrane between both NF tested is the NF90. Furthermore with the NF90 membrane F⁻ level concentration after filtration is sufficient to maintain a prophylactic benefit effect under human health to the permeate (F⁻ concentration situated between 0.8 and 1.5 mg L⁻¹). On the contrary the NF270 membrane shows too high F⁻ concentration in the permeate specially after 4 h.

We determined also the silt density index (denoted SDI) of the Fatick's water and obtained a value of 3.1. This parameter has become the accepted standard for assessing the suitability of membrane processes, particularly in reverse osmosis and nanofiltration for water desalination where

its value should be lower or equal to 3. The SDI value is merely a measure of the decline in filtration rate of a membrane filter under standard test conditions. In effect the test is an indirect "measure" of all suspended solids, bacterial, and colloidal matter in the water to be treated through an attempt to sacrificially plug a microporous cellulose ester membrane filter. The value obtained means that Fatick water has a low fouling properties for our microporous membranes. This result permit to counter-balance the high roughness obtained for the NF90 membrane because a high roughness is usually associated to a high fouling properties of the membrane material, as recently reported [1,10,31].

5. Conclusion

The aim of the present work was to establish a systematic approach in the range of characterization

of commercial nanofiltration (NF) and low pressure reverse osmosis (LPRO) membranes for a better help to the users. We developed two sorts of characterizations: (i) first *physico-chemicals* in terms of hydrophobicity/hydrophilicity, morphology and topography and (ii) secondly in terms of mass transfer with the determination of pure water and saline solution permeabilities, monovalent (NaCl) and divalent (Na_2SO_4) solutes rejections and molecular weight cut-off determination. A model inspired by the phenomenological approach proposed by Kedem and Katchalsky (KK) and completed by Spiegler (S) will help us to quantify separately both parts of mass transfer occurring, the pure convection and the pure diffusion for three membranes in polyamides, 2 NF and 1 LPRO, denoted NF270, NF90 and BW30, respectively. We have limited our study to low concentration polarization by using diluted solutions (10^{-3} to 10^{-1} M) and high flow rate (4 m s^{-1}) under low conversion (5%) operational conditions to develop a new and original approach to classify and better understand the behavior of the commercialized NF and LPRO membranes under brackish waters in order to guide the users to find a suitable membrane.

This novel integer approach has permitted to check that the NF90 membrane is the more efficient membrane for brackish water defluorination due to its diffusional behavior for salts, its high hydraulic permeability and also its intermediate rejection for F^- . It appears clearly now that the mass transfer behavior occurring in NF dedicated to a selective defluorination must be a NF membrane very similar in its mass transfer behavior to a RO membrane.

Furthermore this membrane shows the higher hydraulic permeability to pure water with $L_p = 14.8 \text{ L h}^{-1} \text{ m}^{-2} \text{ bar}^{-1}$ and the higher hydraulic permeability to a 0.1 M NaCl solution with $L_p' = 5.0 \text{ L h}^{-1} \text{ m}^{-2} \text{ bar}^{-1}$. Its critical pressure is 1.6 bar. The NF90 membrane shows the higher R_a with $298 \pm 10 \text{ nm}$. Then this membrane possess a high fouling properties due to its high

roughness, this parameter should be modified by the supplier for a sustainable development of this membrane for the brackish waters defluorination all over the world.

We have also presented a new and very simple method to determine quickly the MWCO of a microporous membrane. The operational conditions determined for the MWCO is using a Na_2SO_4 solution with a concentration of 10^{-3} M.

Further experiments are now conducted to enlarge our systematic approach to all commercialized NF and LPRO membranes for their classification.

Nomenclature

Φ	polarization factor
θ	contact angle (degree)
C_{conv}	solute concentration due to convection (mol L^{-1})
C_m	solute concentration at the surface membrane
C_{int}	solute concentration inside the membrane (mol L^{-3})
C_p	solute concentration in the permeate (mol L^{-1})
C_0	solute concentration in feed (mol L^{-1})
J_{diff}	solute flux due to diffusion ($\text{mol m}^{-2} \text{ s}^{-1}$)
P_M	solute permeability vs. membrane (L h^{-1})
J_v	solvent flux (L h^{-1})
J_s	solute flux (L h^{-1})
L_p	pure water permeability ($\text{L h}^{-1} \text{ m}^{-2} \text{ bar}^{-1}$)
L_p'	saline solution permeability ($\text{L h}^{-1} \text{ m}^{-2} \text{ bar}^{-1}$)
ΔP	transmembrane pressure (bar)
$\Delta \Pi$	osmotic pressure difference across membrane (bar)
R_{obs}	observed retention (%)
R_{real}	real retention (%)
σ	reflection coefficient
R_a	membrane roughness (nm)
ΔC_s	the concentration difference between each side of the membrane $C_m - C_p$ (mol L^{-1})

Acknowledgements

This work was funded by the Middle East Desalination Research Center (MEDRC), project no. 04-AS005. Lots of thanks to Professor M. Rumeau (University of Montpellier, France) for fruitful discussions and to MM. H. Buisson (VWS US), N. Ngaffour (MEDRC) and H. Suty (Veolia water, Anjou recherche) for logistical help.

References

- [1] N. Hilal, H. Al-Zoubi, N.A. Darwish, A.W. Mohammad and M. Abu Arabi, *Desalination*, 170 (2004) 281.
- [2] J.M. Rovel, State and behaviour of seawater desalination in the future, in: *Proceedings of CHEM-RAWN XV*, 21–23 June 2004, Paris, pp. 22–28.
- [3] H.M. Krieg, S.J. Modise, K. Keizer and H.W.J.P. Neomagus, *Desalination*, 171 (2004) 205–215.
- [4] C.K. Diawara, M.Lô. Sidi, M. Rumeau, M. Pontié and O. Sarr, *J. Membr. Sci.*, 219 (2003) 103.
- [5] K.S. Spiegler and O. Kedem, *Desalination*, 1 (1966) 311.
- [6] S. Jain and S.K. Gupta, *J. Membr. Sci.*, 232 (2004) 45.
- [7] Z.V.P. Murthy and S.K. Gupta, *Desalination*, 109 (1997) 39.
- [8] M. Pontié, H. Buisson, C.K. Diawara and H. Essis-Tome, *Desalination*, 157 (2003) 127.
- [9] R.J. Petersen, Composite membranes, *J. Membr. Sci.*, 83 (1993) 81.
- [10] E.M.V. Hoek, S. Bhattacharjee and M. Elimelech, *Langmuir*, 19 (2003) 4836.
- [11] A. Lhassani, M. Rumeau and D. Benjelloun, *Tribune de l'eau*, 603–605 (1–3) (2000) 100.
- [12] M. Mänttari, T. Pekuri and M. Nyström, *J. Membr. Sci.*, 242 (2004) 107.
- [13] M. Pontié, C.K. Diawara and M. Rumeau, *Desalination*, 151 (2002) 267.
- [14] D. Violleau, H. Essis-Tome, H. Habarou, J.P. Croue and M. Pontié, *Desalination*, 173 (2005) 223.
- [15] A.E. Yaroshchuk, *Adv. Colloid Int. Sci.*, 85 (2000) 193.
- [16] A. Szymczyk and P. Fievet, *J. Membr. Sci.*, 252 (2005) 77.
- [17] C. Menjeaud, M. Pontié and M. Rumeau, *Entropie*, 179 (1993) 13.
- [18] M.H. Sy, P. Sene and S. Diouf, *Société d'Édition de l'association d'enseignement médical des hopitaux de Paris*, 15 (2) (1996) 109.
- [19] Y. Wang and E.J. Reardon, *App. Geochem.*, 16 (2001) 531.
- [20] S. Ghorai and K.K. Pant, *Investigations on the column performance of fluoride adsorption by activated alumina in a fixed bed*, Report, Indian Institute of Technology, 2002.
- [21] M. Srimurali, A. Pragathi and J. Karthikeyan, *Environ. Pollut.*, 99 (1998) 285.
- [22] N.V.R. Mohan Rao and C.S. Bhaskaran, *J. Fluorine Chem.* (1988) 4117.
- [23] C.Y. Hu, S.L. Lo, W.H. Kan and Y.D. Lee, *Water Res.*, 39 (5) (2005) 895.
- [24] M. Pontié, M. Rumeau, M. Ndiaye and C.M. Diop, *Santé*, 6 (1) (1996) 27.
- [25] A. Lhassani, M. Rumeau, D. Benjelloun and M. Pontié, *Water Res.*, 35 (2001) 3260.
- [26] J.J. Schoeman and G.W. Leach, *Water Sci. Technol.*, 19 (1986) 953.
- [27] H. Garmes, F. Persin, J. Sandeaux, G. Pourcelly and M. Mountadar, *Desalination*, 145 (2002) 287.
- [28] L. Durand-Bourlier and J.M. Lainé, *Proc. Membrane Technology Conf.*, New Orleans, 1997, pp. 1–16.
- [29] M. Hichour, F. Persin, J. Sandeaux and C. Gavach, *Sep. Purif. Technol.*, 18 (2000) 1.
- [30] Z. Amor, B. Bariou, N. Nameri, M. Taky, S. Nicolas and A. Elmidaoui, *Desalination*, 133 (2001) 215.
- [31] S. Singh, K.C. Kulbe, T. Matsuura and P. Ramamurthy, *J. Membr. Sci.*, 142 (1998) 111–127.